Pan-cancer analysis on the role of KMT2C expression in tumor progression and immunotherapy

WEI CAO[1*], YAWEN XIE[2*], LI CAI[2,3*], MENGQING WANG[2], ZHUOYING CHEN[2], ZITENG WANG[2], JIAJIA XV[2], YUQING WANG[2], RONG LI[2], XUESONG LIU[2] and WENLIANG WANG[4]

[1]Department of Thoracic Surgery, Second Affiliated Hospital of Anhui Medical University, Hefei, Anhui 230601; [2]Inflammation and Immune Mediated Diseases Laboratory of Anhui Province, School of Pharmacy, Anhui Medical University, Hefei, Anhui 230032, P.R. China; [3]Department of Pathology, School of Basic Medicine, Anhui Medical University, Hefei, Anhui 230032, P.R. China; [4]Institute of Clinical Immunology, First Affiliated Hospital of Anhui Medical University, Hefei, Anhui 230022, P.R. China

Received December 4, 2023; Accepted May 10, 2024

DOI: 10.3892/ol.2024.14577

Abstract. Histone lysine N-methyltransferase 2C (KMT2C) is involved in transcriptional regulation and DNA damage repair. Mutations in KMT2C have been implicated in the progression, metastasis, and drug resistance of multiple cancer types. However, the roles of KMT2C in the regulation of tumor prognosis, immune cell infiltration and the immune microenvironment in these multiple cancer types remain unclear. Therefore, in the present study, data from The Cancer Genome Atlas and Genotype-Tissue Expression databases were used for KMT2C expression analyses. Kaplan-Meier and univariate Cox regression analyses were also performed to investigate the prognostic role of KMT2C. In addition, Gene Set Enrichment Analysis (GSEA) was conducted to study the KMT2C-related signaling pathways. Tumor immune estimation resource 2 and single-sample GSEA were conducted to investigate the correlation between KMT2C expression and immune cell infiltrations, and Spearman's analysis was conducted to study the correlations among KMT2C, tumor mutational burden, microsatellite instability, immune regulators, chemokines and immune receptors. Immunohistochemistry of patient kidney tumor samples was performed to verify the correlation between KMT2C and programmed death-ligand 1 (PD-L1) expression. Finally, RNA interference, wound healing and colony formation assays were conducted to evaluate the effects of KMT2C expression on cell proliferation and metastasis. The results of the present study demonstrated that KMT2C was highly expressed in multiple cancer types, was a protective factor in kidney renal clear cell carcinoma and ovarian serous cystadenocarcinoma, and a risk factor for lung squamous cell carcinoma and uveal melanoma. In addition, KMT2C levels were negatively correlated with immune-activated pathways and the infiltration of immune cells, and positively correlated with inhibitory immune factors and tumor angiogenesis. Patients with low KMT2C expression had higher objective response rates to immunotherapy, and drug sensitivity analysis indicated that topoisomerase, histone deacetylase, DOT1-like histone H3K79 methyltransferase and G9A nuclear histone lysine methyltransferase inhibitors could potentially be used to treat tumors with high KMT2C expression levels. Finally, the KMT2C and PD-L1 expression levels were shown to be positively correlated, and KMT2C knockdown markedly promoted the proliferation and invasion capacities of A549 cells. In conclusion, the present study revealed that low KMT2C expression may be a promising biomarker for predicting the response of patients with cancer to immunotherapy. Conversely, high KMT2C expression was shown to promote tumor angiogenesis, which may contribute to the formation of the immunosuppressive tumor microenvironment.

Correspondence to: Dr Wenliang Wang, Institute of Clinical Immunology, First Affiliated Hospital of Anhui Medical University, 218 Jixi Road, Hefei, Anhui 230022, P. R. China
E-mail: wwlanhui@126.com

Dr Xuesong Liu, Inflammation and Immune Mediated Diseases Laboratory of Anhui Province, School of Pharmacy, Anhui Medical University, 81 Meishan Road, Hefei, Anhui 230032, P.R. China
E-mail: chemxsliu@126.com

*Contributed equally

Key words: histone lysine N-methyltransferase 2C, pan-cancer, immunotherapy biomarker, tumor microenvironment

Introduction

The development of cancer immunotherapy, particularly immune checkpoint blockades, has revolutionized cancer treatment (1-3). Immunotherapy activates the natural defense system of the host, which identifies and eliminates tumor cells. This strategy has emerged as an effective treatment with unparalleled and synergistic survival benefits in multiple cancer types, such as melanoma and non-small cell lung carcinoma (4-6). At present, 11 immune checkpoint inhibitors (ICIs) have been clinically approved for the treatment of 16 malignant diseases (7,8). However, overcoming treatment resistance is becoming increasingly challenging, and fewer than one-third of patients with cancer achieve significant and long-term responses to cancer immunotherapy (9-11). Thus,

there is an urgent need to identify predictive biomarkers of immunotherapy responses.

The histone lysine N-methyltransferase 2 (KMT2) family of proteins regulates the expression of specific regions of the genome by methylating histone H3 lysine K4 (H3K4). This modification leads to chromatin remodeling and DNA accessibility, which are involved in the occurrence, progression and immune tolerance of a number of cancer type, such as breast and prostate cancer (12,13). The KMT2 family of proteins includes KMT2A, KMT2B, KMT2C and KMT2D. KMT2A and KMT2B dimethylate and trimethylate chromatin at the promoter regions and polycomb response elements of genes, while KMT2C and KMT2D monomethylate H3K4 at the gene enhancer regions (14-17).

KMT2C (also known as MLL3) regulates DNA damage response and repair by directly binding to sites of DNA damage and mediating histone methylation. This histone modification process relaxes the chromosomal structure near the damaged DNA, enabling other key proteins to access the damaged sites and repair the damage (18,19). KMT2-encoding genes are frequently mutated in a number of cancer types, such as small cell lung and breast cancer (20-22). These genes are closely related to the occurrence and development of multiple tumors, and significantly affect the clinical eradication of tumors, particularly with immunotherapy (20-22). Zhang and Huang (23) reported that mutations targeting the KMT2 family of proteins may be predictive biomarkers of a favorable response to treatment with ICIs in multiple cancer types, such as melanoma, bladder, uterine, and lung carcinomas. Compared with patients harboring wild-type *KMT2A/C*, those with *KMT2A/C* mutations achieved higher overall survival (OS), progression-free survival, objective response rate (ORR) and durable clinical benefits upon ICI treatment (24). However, the relationship between KMT2C expression in tumor immune infiltration and the predicted immunotherapeutic response remains unclear due to the publication of few comprehensive pan-cancer studies to date.

In the present study, the relationship between KMT2C expression and various tumor-associated parameters were evaluated in a pan-cancer setting. The present study will contribute to the understanding of the role of KMT2C in tumor progression and immunotherapy.

Materials and methods

Data collection. The workflow of the present study is shown in Fig. 1. The Cancer Genome Atlas (TCGA) pan-cancer dataset were downloaded from the Genotype-Tissue Expression project (https://xenabrowser.net/datapages/) and the UCSC Xena database (https://xenabrowser.net/datapages/). Data on the following cancer types were included in the present study: Adrenocortical carcinoma (ACC), bladder urothelial carcinoma (BLCA), breast invasive carcinoma (BRCA), cervical squamous cell carcinoma and endocervical adenocarcinoma (CESC), cholangiocarcinoma (CHOL), colon adenocarcinoma (COAD), large B cell lymphoma (DLBC), esophageal cancer (ESCA), glioblastoma (GBM), head and neck squamous cell carcinoma (HNSC), kidney chromophobe (KICH), kidney renal clear cell carcinoma (KIRC), kidney renal papillary cell carcinoma, acute myeloid leukemia (LAML), low grade glioma (LGG), liver hepatocellular carcinoma (LIHC), lung adenocarcinoma (LUAD), lung squamous cell carcinoma (LUSC), mesothelioma, ovarian serous cystadenocarcinoma (OV), pancreatic adenocarcinoma (PAAD), pheochromocytoma and paraganglioma (PCPG), prostate adenocarcinoma (PRAD), rectal adenocarcinoma (READ), sarcoma (SARC), skin cutaneous melanoma (SKCM), stomach adenocarcinoma (STAD), testicular germ cell tumors (TGCT), thyroid carcinoma (THCA), thymoma (THYM), uterine corpus endometrial carcinoma (UCEC), uterine carcinosarcoma (UCS) and uveal melanoma (UVM). The transcriptomic, CRISPR-Cas9 and small interfering RNA data generated using cancer cell lines were downloaded from the Cancer Cell Line Encyclopedia (CCLE) website (https://sites.broadinstitute.org/ccle/). Immunotherapy cohort data were downloaded from the Gene Expression Omnibus (https://www.ncbi.nlm.nih.gov/geo/).

Prognostic analysis. The prognosis data including OS, disease-specific survival (DSS), disease-free interval (DFI) and progression-free interval (PFI) were downloaded from the UCSC Xena database (xenabrowser.net/datapages/). Kaplan-Meier and univariate Cox regression analyses were conducted to calculate the association between KMT2C expression and the pan-cancer OS, DSS, DFI and PFI. The samples were divided into high and low expression according to the optimal cut-off point. Multivariate Cox regression analyses were also conducted to calculate the association between KMT2C expression and the pan-cancer OS. Univariate Cox analysis was performed using the UCSC-Xena-Shiny website (https://shiny.hiplot-academic.com/ucsc-xena-shiny/). Multivariate Cox analyses were performed using the R package, 'survival'. Kaplan-Meier analyses were performed using the R packages, 'survival' and 'survminer' (R 4.2.0; r-project.org/).

Gene set enrichment analysis (GSEA). TCGA patient samples were divided into two groups based on the KMT2C expression levels. The samples were arranged in expression order and the top 30% of the samples were defined as the high KMT2C expression group and the bottom 30% as the low KMT2C expression group, with the remainder excluded from analysis (25). The gene sets were downloaded from the MsigDB database (https://www.gsea-msigdb.org/gsea/msigdb). GSEA was performed using the R package, 'ClusterProfiler'.

Single-cell analysis. Single-cell analysis was performed using Tumor Immune Single-cell Hub (TISCH) web tool (26). Results were visualized using the R package, 'ggplot2'. The single-cell hepatocellular carcinoma dataset (dataset ID, SCDS0000020) was also analyzed using the Cell-omics Data Coordinate Platform (CDCP; https://db.cngb.org/cdcp/dataset/SCDS0000020/).

Chemotherapy sensitivity analysis. The correlation between KMT2C expression and the sensitivity to small molecule inhibitors was investigated using the CMap (https://portals.broadinstitute.org/cmap/) and SPIED3 (92.205.225.222/HGNC-SPIED3-QF.py) web tools (27). Drug sensitivity and gene expression data were obtained from experiments with cancer cell lines and downloaded from the

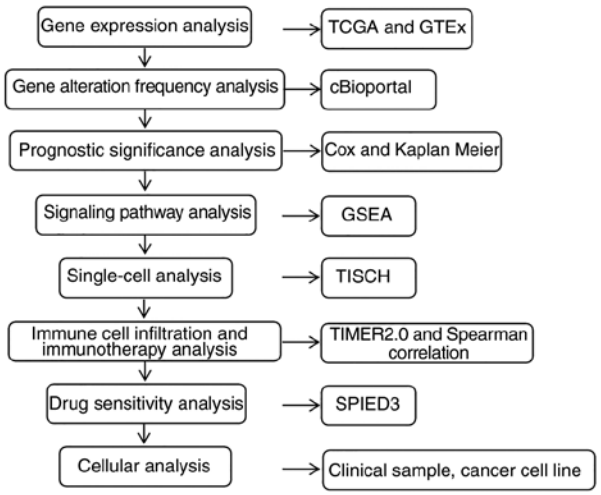

Figure 1. Experimental flowchart of the present study. TCGA, The Cancer Genome Atlas; GTEx, Genotype-Tissue Expression; GSEA, Gene Set Enrichment Analysis.

GDSC (https://www.cancerrxgene.org/) database (28). The correlation between drug sensitivity and gene expression was analyzed using the Spearman's test.

Analysis of the tumor microenvironment (TME). Single-sample (ss)GSEA was conducted to calculate the tumor immune cell infiltration scores (29) using R 4.2.0. A Spearman's correlation analysis was performed to investigate the correlation between tumor immune cell infiltration scores, immune checkpoint-related genes and KMT2C expression (R 4.2.0). The TIMER2 webtool (http://timer.cistrome.org/) was used to evaluate the relationship between KMT2C expression and tumor immune cell infiltration.

Immunotherapy response prediction analyses. Immunotherapy response prediction analyses of KMT2C expression were performed using the Tumor Immune Dysfunction and Exclusion (TIDE) computational method (http://tide.dfci.harvard.edu) (30). Correlations between KMT2C expression and tumor mutational burden (TMB) and microsatellite instability (MSI) were analyzed using Spearman's correlation test using R 4.2.0. IMvigor210 (31), PRJEB23709 (32), PRJNA482620 (33) and PRJEB25780 (34) immunotherapy cohort datasets were used to analyze and identify the predictive value of KMT2C.

Immunohistochemistry. Paraffin-embedded kidney tumor tissue samples were obtained from patients treated at the Second Affiliated Hospital of Anhui Medical University (Hefei, China) with informed consent from May 2019 to March 2022. The inclusion criteria were as follows: diagnosed with renal cancer, not receiving treatment, and the patient is willing to provide pathology sections for study. Tumors were staged according to the 8th edition of the INM classification of malignant tumors (35). The basic patient clinical information is provided in Table SI. All experiments were approved by the Medical Ethics Committee of the Second Affiliated Hospital of Anhui Medical University (approval no. 81220282). Immunohistochemistry was performed by Servicebio Co., Ltd. 4% Paraformaldehyde Fix Solution (Beyotime Institute of Biotechnology; cat. no. P0099) fixed (room temperature, 24 h) and paraffin-embedded kidney tumor tissue were cut into 5-μm-thick sections, dried, deparaffinized and dehydrated in a graded ethanol series. The antigen was retrieved by microwave method using sodium citrate (10 mM, pH 6.0) for 20 min, and then washed by phosphate buffered saline (PBS) 3 times. The tissue sections were treated with 1% hydrogen peroxide (Beyotime, P0100A) for 10 min to block endogenous tissue peroxidase activity and treated with goat serum (Beyotime, C0265) for 1 h at room temperature to block non-specific protein binding. The slides were incubated with rabbit monoclonal anti-human PD-L1 antibody (Abcam, ab205921, 1:500) or rabbit polyclonal anti-human KMT2C antibody (absin, abs113638 1:200) overnight at 4˚C. Then, the slides were incubated with the Universal kits (ZSGB-BIO; cat. no. PV-6000) at room temperature for 20 min. The slides were washed with PBS and colored with 3,3'-diaminobenzidine substrate kit (ZSGB-BIO, ZLI-9017) for 5 min. Then, the slides were counterstained with hematoxylin staining solution (ZSGB-BIO, ZLI-9610) at room temperature for 1 min, and visualized with a light microscope (Nikon, ECLIPSE Ti2). The tumor proportion score (TPS) was used to evaluate the expression of programmed death-ligand 1 (PD-L1) in tumor samples. The TPS was calculated as follows: TPS=(number of tumor cells with positive PD-L1 membrane staining/total number of tumor cells) x100%. The average optical density (representing KMT2C expression) was calculated using ImageJ1.53t software (National Institutes of Health).

In vitro cellular assays. The A549 and H1975 human lung cancer cell lines was purchased from Nanjing CoBioer Biotechnology Co., Ltd. A549 cells were cultured in DMEM (Corning, Inc.) supplemented with 10% (v/v) fetal bovine serum (FBS; ExCell, Inc.) and 1% (v/v) penicillin/streptomycin. H1975 cells were cultured in RPMI-1640 (Corning, Inc.) supplemented with 10% (v/v) FBS and 1% (v/v) penicillin/streptomycin. The immortalized human umbilical vein endothelial cell (HUVEC) line was purchased from Xiamen Immocell Biotechnology Co., Ltd (IM-H205). and cultured in human umbilical vein endothelial cell medium (HUVEC-90011; Cyagen Biosciences, Inc.).

KMT2C knockdown cell line construction. KMT2C knockdown pLKO.1 plasmids were purchased from Shanghai GenePharma Co., Ltd. Plasmids (pLKO.1:pSPAX.2: pMD2G=2:2:1) were transfected into 293T with polyethylenimine (YEASEN, 40815ES03, 1 μg/ml). After 48 h, the lentivirus was collected. When the cells were in the logarithmic phase, 1x10^5 cells were seeded into a 6-well plate and 1 ml lentivirus (MOI=10) and 1.5 μl 10 μg/μl polybrene(absin) were added at 37˚C for 24 h. The medium was replaced with fresh medium after 24 h. After 48 h, 1 μg/μl puromycin was added to the medium for screening. The transfection efficiency was examined by immunoblotting analysis. The short hairpin (sh)RNA sequences used were as follows: shNC, 5'-TTCTCC GAACGTGTCACGT-3'; sh1, 5'-CGATCTCCTCAGCAGAAT ATA-3'; and sh2, 5'-CTGAGCTCACTACAGATTATA-3'.

Immunoblotting analysis. Proteins from the cells extracted using RIPA buffer (Beyotime, P0013B) and quantified by the

Pierce BCA Protein assay (Thermo, 23225), and 40 ug of each sample was loaded on Nitrocellulose (0.45 μm) membrane (Bio-Rad, 1620115), and was blocked by 5% skim milk 1 h, then TBST (1% TWEEN 20) wash 3 times for 15 min. Next, the membrane was incubated with the primary antibody KMT2C (absin, abs113664, dilution: 1:1,000) and anti-β-Actin Monoclonal Antibody (absin, abs830031, dilution: 1:1,000) at 4˚C overnight and followed by peroxidase-conjugated secondary antibody (HUABIO, HA1008, dilution: 1:5,000) for 1 h. at 37˚C. Protein bands were visualized by an enhanced chemiluminescent detection kit (Thermo, A38554) with ChemiDoc XRS+ System (Bio-Rad, USA).

Reverse transcription-quantitative polymerase chain reaction. The RNA extraction kit (AG21101; Accurate Biology) was used to extract the total cellular RNA and the reverse transcription kit (AG11706; Accurate Biology) to reverse transcription. RT-qPCR) reactions were run on a Bio-Rad IQ 5 RT-PCR detection system using SYBR Green Premix Pro Taq HS qPCR Kit (AG11701; Accurate Biology).The primers were ordered from Biosune company, having the following sequences: Forward (F)_KMT2C, 5'-CCTCCCTCCCAACAC CACCTC-3'; Reverse(R)_KMT2C, 5'-TCTGGATACCTG CTCACTTCTACCC-3';F_GAPDH, 5'-GAGAAGTATGAC AACAGCCTCAA-3'; and R_GAPDH, 5'-GCCATCACGCCA CAGTTT-3'. Use the reverse transcription kit AG11706 reverse recording reaction: instantaneous separation after mixing; the procedure is 37˚C/15 min, 85˚C 5 sec, 4˚C. Then the target primer and template cDNA were then diluted 40 times with the AG11701 SYBRGreen ProTaq HS pre-mixed qPCR kit (10 μl system) with 3 complex wells for each sample. GAPDH was used as the internal reference gene. The thermocycling conditions were as follows: samples were incubated at 95˚C for 30 sec, followed by 40 cycles at 95˚C for 5 sec and 60˚C for 30 sec. The results were analyzed by the 2-ΔΔCq method (36).

Colony formation and wound healing assays. Colony formation and wound healing assays were conducted as previously reported (37). For the colony formation assay, $1x10^4$ cells were seeded into a 6-well plate with 2 ml complete medium and cultured for ~2 weeks. Then, cells fixed with 4% paraformaldehyde 20 min at room temperature and stained by 0.1% crystal violet 20 min at room temperature. The number of colonies were calculated using ImageJ software. The number of cells over 60 was defined as a clone. For the cell migration assay, cells were grown to 100% confluency and a wound gap was created by a scratch instrument. The medium was replaced with medium containing 0.1% FBS, and images were collected using a light microscope EVOS XL Core Cell Imaging System (Thermo Fisher Scientific, Inc.) on days 0 and 7 after scratch formation. The gap closure was calculated using ImageJ software 1.53t.

Anti-proliferation assay. Small molecular inhibitors SN-38 (HY-13704), vorinostat (HY-10221), UNC0224 (HY-10929), SGC0946 (HY-15650) were purchased from MedChemExpress (Shanghai, China). The cells were plated in 96-well plate (3,000 cells/well) and medium is replaced with DMEM (Corning, Inc.) containing different concentrations (10, 3, 1, 0.3, 0.1, 0.03, 0.010, 0.003, 0.001 μM) of small molecule inhibitors, and incubated in 37˚C and 5% CO_2. After 72 h, 10 μl CCK8 (C0038, Beyotime Institute of Biotechnology) were added in per well and incubate at 37˚C for 30 min. Detection (450 nm) was performed with a microplate reader (Thermo Fisher Scientific, Inc.).

Statistical analysis. All data were statistically analyzed using R software 4.2.0 (https://www.r-project.org/). Kaplan-Meier and univariate Cox regression analyses were conducted for survival analysis. Statistically significant correlations was determined using the Spearman's test. Analyses of KMT2C expression in cancer and normal tissues were conducted using unpaired Student's t-test. One way ANOVA and Bonferroni was used for multi-group data comparisons. All P-values were two-sided, and $P<0.05$ was considered to indicate a statistically significant difference.

Results

Analysis of pan-cancer KMT2C expression. KMT2C expression in The Cancer Genome Atlas (TCGA) pan-cancer dataset was evaluated. KMT2C was highly expressed in BRCA, CHOL, ESCA, GBM, KICH, LAML, LGG, PAAD, PRAD and STAD tumor samples. By contrast, low KMT2C expression was observed in ACC, BLCA, CESC, COAD, LUAD, LUSC, OV, SKCM, TGCT, THCA, THYM, UCEC and UCS (Fig. 2A). Analysis of KMT2C expression in paired tumor and normal pan-cancer tissues revealed that KMT2C was highly expressed in CHOL, LIHC and KICH tumor tissues, whereas its expression was low in COAD and THCA tumor tissues (Figs. 2B-E and S1A). The expression of KMT2C at different tumor stages was further investigated, and it was demonstrated that the expression varied significantly at the different stages of COAD, KIRC, OV and STAD (Fig. S1B-E).

Next, the expression of KMT2C in different cancer cell lines was investigated using CCLE datasets. KMT2C was highly expressed in myeloma, lymphoma, breast cancer, gastric cancer and leukemia cell lines, whereas low expression was observed in teratoma, liposarcoma, bile duct cancer, head and neck cancer and cervical cancer cell lines (Fig. 2F). CRISPR/Cas9 data showed that *KMT2C* knock-out inhibited the proliferation of teratoma, rhabdoid, lymphoma and myeloma cells (Fig. 2G). Similarly, RNA interference analyses indicated that silencing of *KMT2C* expression inhibited the proliferation of myeloma and rhabdoid cells (Fig. S1F). The genomic alterations in *KMT2C* in pan-cancer samples were also analyzed. The results indicated that the cancer types with frequencies >20% were bladder cancer and melanoma (Fig. S2A). The effect of *KMT2C* mutations on its protein expression were further investigated. The results showed that the presence or absence of a *KMT2C* mutation did not affect its protein expression (Fig. S2B).

Prognostic significance of KMT2C. The pan-cancer prognostic value of KMT2C was investigated using univariate Cox regression analysis. The OS and PFI results indicated that KMT2C acted as a protective factor for patients with KIRC and OV but was a risk factor for patients with LUSC and UVM. The DSS results indicated that KMT2C acted as a protective factor in patients with KIRC (Fig. 3A). Next, the prognostic value

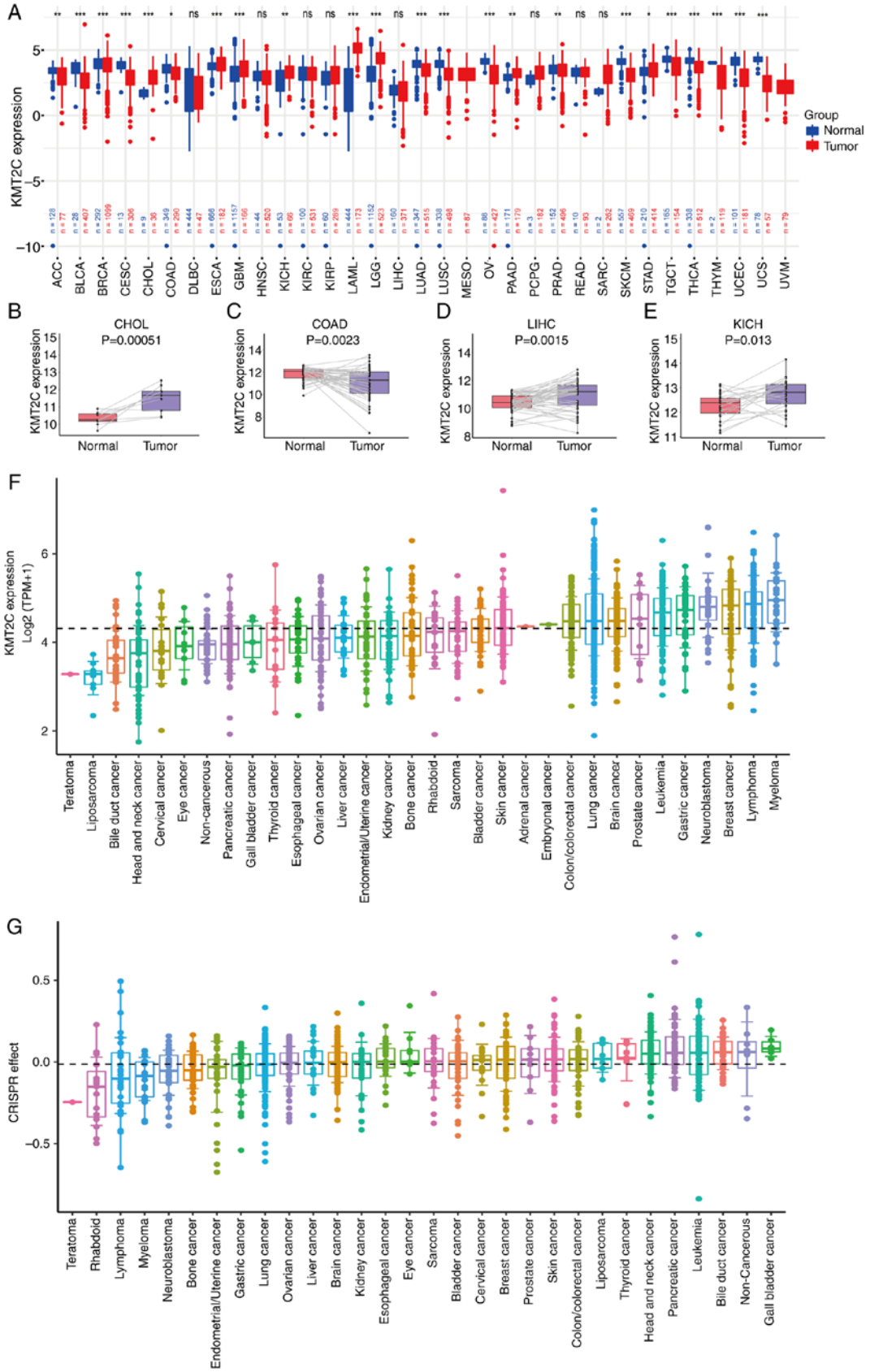

Figure 2. Expression analysis of KMT2C in pan-cancer. (A) Pan-cancer analysis of KMT2C expression in tumor and normal tissues from TCGA and Genotype-Tissue Expression databases. (B) Analysis of KMT2C expression in paired CHOL tumor and adjacent normal tissues. (C) Analysis of KMT2C expression in paired COAD tumor and adjacent normal tissues. (D) Analysis of KMT2C expression in paired LIHC tumor and adjacent normal tissues. (E) Analysis of KMT2C expression in paired KICH tumor and adjacent normal tissues. (F) Pan-cancer analysis of KMT2C expression in cancer cell lines from the CCLE. The threshold lines represent the mean KMT2C expression in all cells. (G) Effect of CRISPR/Cas9 knockout on KMT2C expression on cancer cell lines (data from CCLE). *P<0.05, **P<0.01, ***P<0.001. CCLE, Cancer Cell Line Encyclopedia; KMT2C, histone lysine N-methyltransferase 2C; ns, not significant; TCGA, The Cancer Genome Atlas; TMP, transcripts per million; CHOL, cholangiocarcinoma; COAD, colon adenocarcinoma; LIHC, liver hepatocellular carcinoma; KICH, kidney chromophobe.

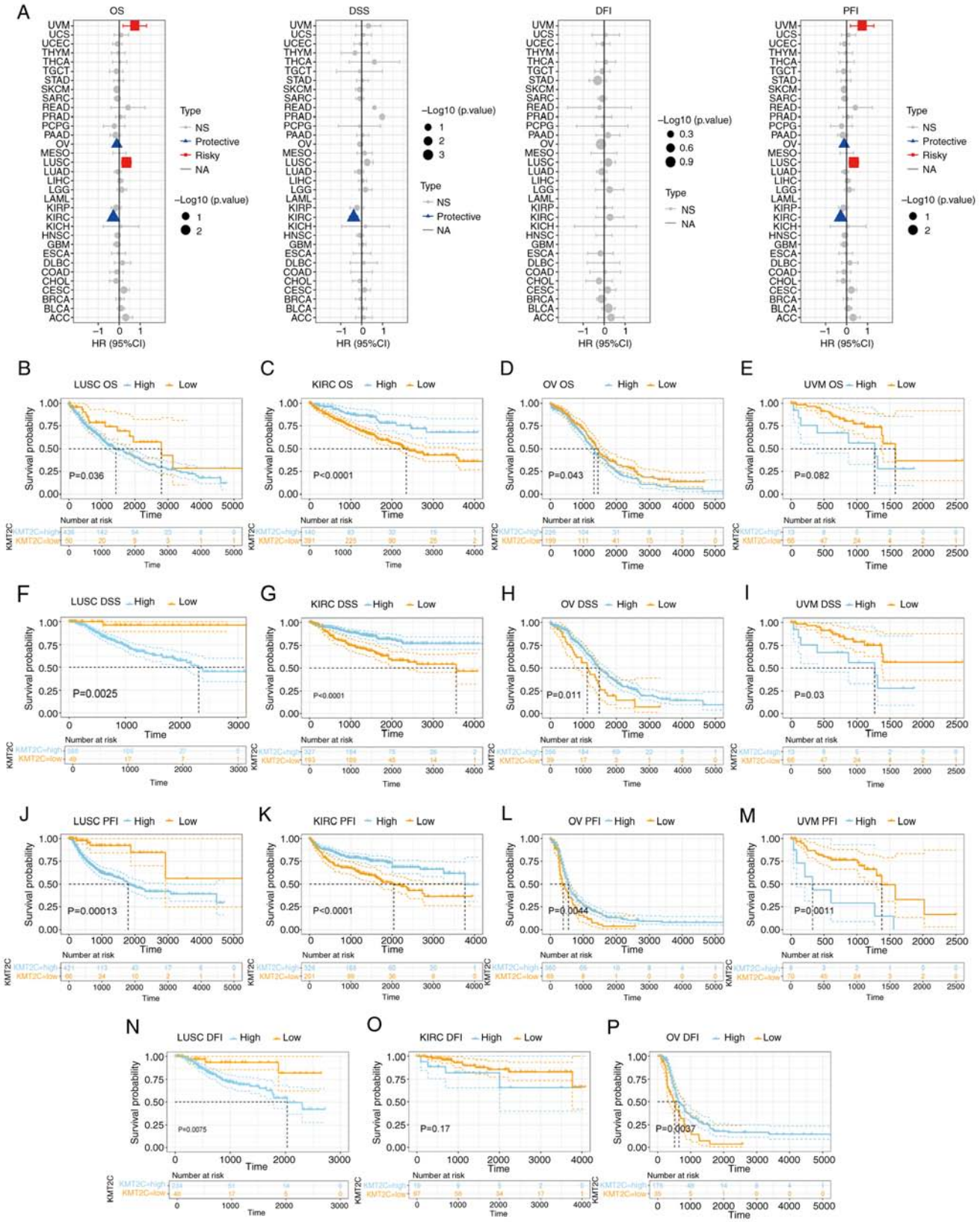

Figure 3. Prognostic significance of KMT2C expression. (A) Univariate Cox regression analysis of the effect of KMT2C on OS, DSS, DFI and PFI in pan-cancer. (B) Kaplan-Meier analysis of the effect of KMT2C on OS in LUSC. (C) Kaplan-Meier analysis of the effect of KMT2C on OS in KIRC. (D) Kaplan-Meier analysis of the effect of KMT2C on OS in OV. (E) Kaplan-Meier analysis of the effect of KMT2C on OS in UVM. (F) Kaplan-Meier analysis of the effect of KMT2C on DSS in LUSC. (G) Kaplan-Meier analysis of the effect of KMT2C on DSS in KIRC. (H) Kaplan-Meier analysis of the effect of KMT2C on DSS in OV. (I) Kaplan-Meier analysis of the effect of KMT2C on DSS in UVM. (J) Kaplan-Meier analysis of the effect of KMT2C on DFI in LUSC. (K) Kaplan-Meier analysis of the effect of KMT2C on DFI in KIRC. (L) Kaplan-Meier analysis of the effect of KMT2C on DFI in OV. (M) Kaplan-Meier analysis of the effect of KMT2C on DFI in UVM. (N) Kaplan-Meier analysis of the effect of KMT2C on PFI in LUSC. (O) Kaplan-Meier analysis of the effect of KMT2C on PFI in KIRC. (P) Kaplan-Meier analysis of the effect of KMT2C on PFI in OV. CI, confidence interval; DFI, disease-free interval; DSS, disease specific survival; HR, hazard ratio; KMT2C, histone lysine N-methyltransferase 2C; NA, not applicable; NS, not significant; OS, overall survival; PFI, progression free interval. KIRC, kidney renal clear cell carcinoma; LUSC, lung squamous cell carcinoma; OV, ovarian serous cystadenocarcinoma; UVM, uveal melanoma.

of KMT2C in KIRC, LUSC, OV and UVM was investigated using Kaplan-Meier analysis. The OS results showed that elevated KMT2C expression was related to a shorter OS time in LUSC and OV, and a longer OS time in KIRC (Fig. 3B-E). The DSS results showed that elevated KMT2C expression was positively associated with a shorter DSS time in LUSC and UVM, but a longer DSS time in KIRC and OV (Fig. 3F-I). The PFI results showed that elevated KMT2C was related to a shorter PFI in LUSC and UVM, and a longer PFI in KIRC and OV (Fig. 3J-M). The DFI results showed that elevated KMT2C levels were positively associated with a shorter DFI in LUSC, and a longer DFI in OV (Fig. 3N-P). The pan-cancer prognostic value of KMT2C was also investigated using multivariate Cox regression analysis. KMT2C acted as a risk factor for HNSC, KIRC and LUAD (Table SII). The different prognostic roles of KMT2C in different cancer types may be regulated by the TME.

Pan-cancer GSEA of KMT2C. The signaling pathways through which KMT2C may be involved in cancer was investigated using GSEA. The expression of KMT2C was highly and negatively correlated with immune-activated pathways, such as those associated with tumor necrosis factor (TNF)-α, interferon (IFN)-γ and IFN-α signaling, the pro-inflammatory response and allograft rejection, particularly in BLCA, BRCA, ESCA, HNSC, LUAD, LUSC, PAAD and READ (Fig. 4A). These results suggested that high expression of KMT2C may be a potential marker of the immunosuppressive TME. It was further observed that KMT2C expression was significantly positively correlated with activation of signaling pathways implicated in the response to ultraviolet radiation, reactive oxygen species, oxidative phosphorylation, MYC signaling, mitotic spindle and DNA repair, consistent with the function of KMT2C as a DNA damage regulator (Fig. 4A). Since tumor angiogenesis is an important factor in tumor progression and has a key role in tumor growth, metastasis and resistance to chemotherapy and immunotherapy, it was also found that KMT2C expression was significantly associated with the neovascularization process, angiogenesis and the VEGFA/VEGFR2 signaling pathway (Fig. 4B). To verify the effect of KMT2C on angiogenesis, a HUEVC angiogenesis experiment was performed. The results showed that knockdown of KMT2C inhibited angiogenesis to a certain extent (Fig. S3A and B).

Single-cell pan-cancer analysis of KMT2C expression. Next, the expression of KMT2C in tumor and stromal cells from 58 single-cell cancer sample datasets was investigated using the TISCH web tool. The results showed that KMT2C was expressed in immune cells, endothelial cells (ECs), fibroblasts and malignant cells (Fig. 5). In the GSE146771 colon cancer dataset, which contained 54,285 single-cell samples from 18 patients, KMT2C was widely expressed in a range of immune cells, including B cells, conventional $CD4^+$ T cells (CD4Tconv), functional $CD8^+$ T cells (CD8T), exhausted CD8T cells (CD8Tex), monocytes, macrophages, natural killer (NK) cells, proliferating T cells (Tprolif) and regulatory T cells (Tregs). In the GSE131928 glioma cancer dataset, which contained 7,930 single-cell samples from 35 patients, KMT2C was widely expressed in astrocyte-like malignant cells, CD8Tex, malignant cells, monocytes, macrophages, oligodendrocytes and oligodendrocyte progenitor-like malignant cells. Finally, in the GSE120575 melanoma dataset, which contained 16,291 single-cell samples from 32 patients, KMT2C was widely expressed in B cells, CD4Tconv, CD8T, CD8Tex, dendritic cells (DCs), monocytes, macrophages, NK cells, Tprolif and Tregs. Together, these results indicated that KMT2C was widely expressed in the TME (Fig. 5). The expression of KMT2C in hepatocellular carcinoma was also investigated using the CDCP tool. KMT2C was widely expressed in T, NK and myeloid cells (Fig. S4).

Immune cell infiltration analysis. To investigate the relationship between KMT2C expression and tumor immunity, the correlation between KMT2C levels and tumor immune cell infiltration was investigated using ssGSEA. The expression of KMT2C was positively correlated with the levels of infiltrated type 2 T helper (Th2) cells, memory B cells, immature DCs, eosinophils and effector memory $CD4^+$ T cells in most cancer types and negatively correlated with the infiltration levels of Th17 cells, Th1 cells, plasmacytoid (p)DCs, Natural killer T cells (NK-T), monocytes, myeloid-derived suppressor cells (MDSCs), macrophages, γδ T cells, central memory $CD4^+$ T cells, $CD56^{dim}$ and $CD56^{bright}$ NK cells, activated DCs and activated $CD8^+$ T cells (Fig. 6A). In addition, the relationship between KMT2C expression and tumor immune cell infiltration was investigated using data from the TIMER2 database. The expression of KMT2C was positively correlated with the infiltration levels of B cells, cancer-associated fibroblasts (CAFs), DCs, ECs, M2 macrophages, mast cells, monocytes, neutrophils, $CD4^+$ T cells and Tregs in most of the cancer types in TCGA, and negatively correlated with the infiltration levels of pDCs, M1 macrophages, NK cells, γδ T cells, NKT cells and Th1 cells in most of the cancer types (Fig. S5A). The potential correlation between KMT2C expression and immune checkpoint genes, chemokines and receptors were further investigated. KMT2C expression was significantly positively correlated with the upregulation of immune inhibitory genes, such as *EDNRB, VEGFA, KDR, CD274, TGFBR1, ADORA2A, CD276, HMGB1, ENTPD1* and *BTN3A1*, in most cancer types, and was significantly negatively correlated with the upregulation of immune stimulatory genes, such as *TNFRSF4* and *TNFRSF18*, in multiple types of cancer (Fig. 6B). It was also found that KMT2C expression was significantly positively correlated with the expression of chemokines CXCL12, CXCL16, CX3CL1 and CCL28, and most immune receptors (Fig. S5B and C). Collectively, these results indicated that KMT2C expression was significantly correlated with various components of the immunosuppressive TME.

Predictive role of KMT2C in cancer immunotherapy. To further investigate the relationship between KMT2C expression and T cell function, the role of KMT2C in T cell killing was reevaluated using published data (38). Knockout of *KMT2C* expression improved T cell killing, implicating KMT2C as a potential immunotherapeutic biomarker (Fig. S6A). To verify the role of KMT2C in predicting the efficacy of ICIs in patients, the correlation between KMT2C expression, TMB and MSI were assessed. The results demonstrated that KMT2C was significantly negatively correlated with the TMB

Figure 4. GSEA of histone lysine N-methyltransferase 2C in pan-cancer. (A) Hallmark gene set (h.all.v7.4.symbols.gmt) and the WikiPathways subset of CP (c2.cp.wikipathways.v2022.1.Hs.symbols.gmt) were used to calculate the NES and FDR. (B) The WikiPathways subset of CP (c2.cp.wikipathways.v2022.1.Hs.symbols.gmt) were used to calculate the NES and FDR. The results were visualized using the R package, 'ggplot2'. *P<0.05, **P<0.01. FDR, false discovery rate; NES, normalized enrichment score.

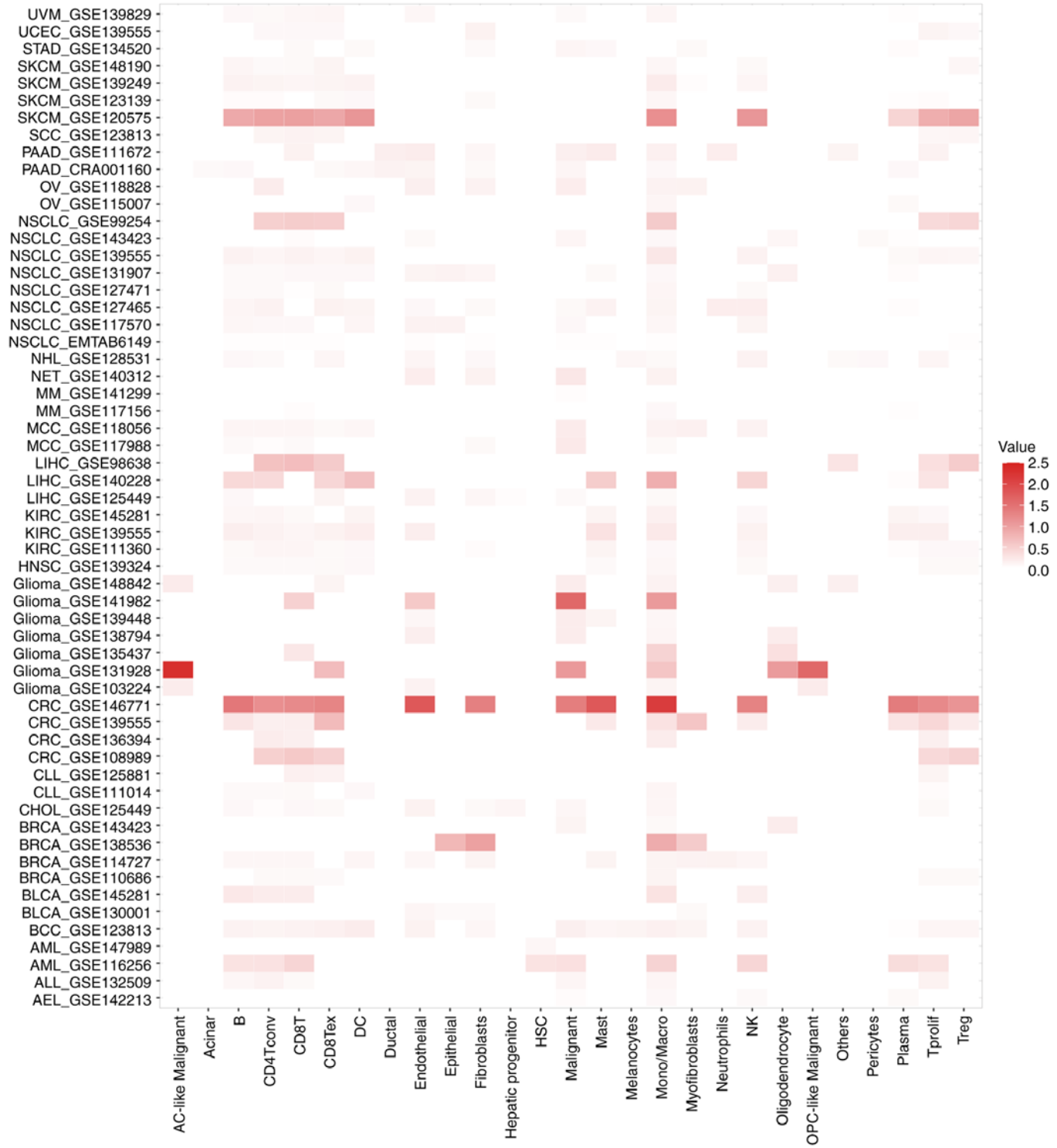

Figure 5. Single-cell analysis of histone lysine N-methyltransferase 2C expression in 33 cell types, using data from the TISCH single-cell database.

in BRCA, COAD, DLBC, KICH, KIRC, PAAD, STAD, TGCT and THCA, but positively correlated with the TMB in HNSC, PRAD and THYM (Fig. 7A). Furthermore, KMT2C expression was significantly negatively correlated with MSI in ACC, BRCA, COAD, HNSC, KIRC, LIHC, PAAD, PCPG, PRAD, READ, SARC, SKCM, STAD, TGCT, THCA and THYM (Fig. 7B). In addition, TIDE was employed to investigate the correlation between KMT2C levels and the response to immunotherapy and to compare the predictive value of KMT2C with the values of other standardized cancer biomarkers. The area under the receiver operator characteristic curve for KMT2C was >0.5 in 12 immunotherapy cohorts, suggesting that the KMT2C level exhibited a higher predictive value than the TMB, T cell clonality (T.Clonality) and B cell clonality (B.Clonality) biomarkers (Fig. 7C).

Several clinical databases were searched to investigate the role of KMT2C in immunotherapy. The IMvigor210 cohort included the transcriptomic and immunophenotypic profiles of

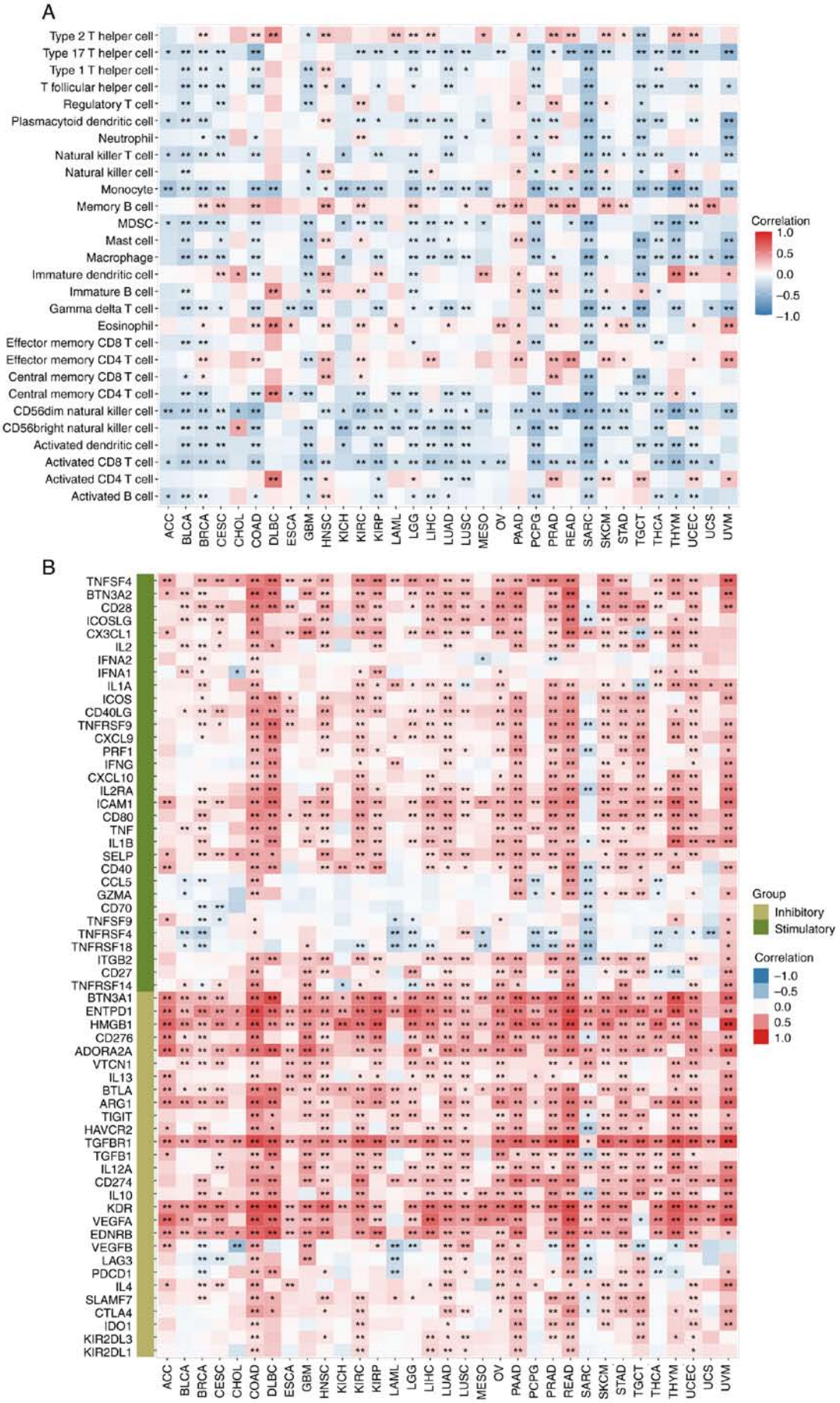

Figure 6. Immune cell infiltration analysis. (A) Correlations between KMT2C expression and the infiltration scores of 28 immune cells in pan-cancer. (B) Correlations between KMT2C expression and the expression of immune regulators in pan-cancer. *P<0.05, **P<0.01. KMT2C, histone lysine N-methyltransferase 2C.

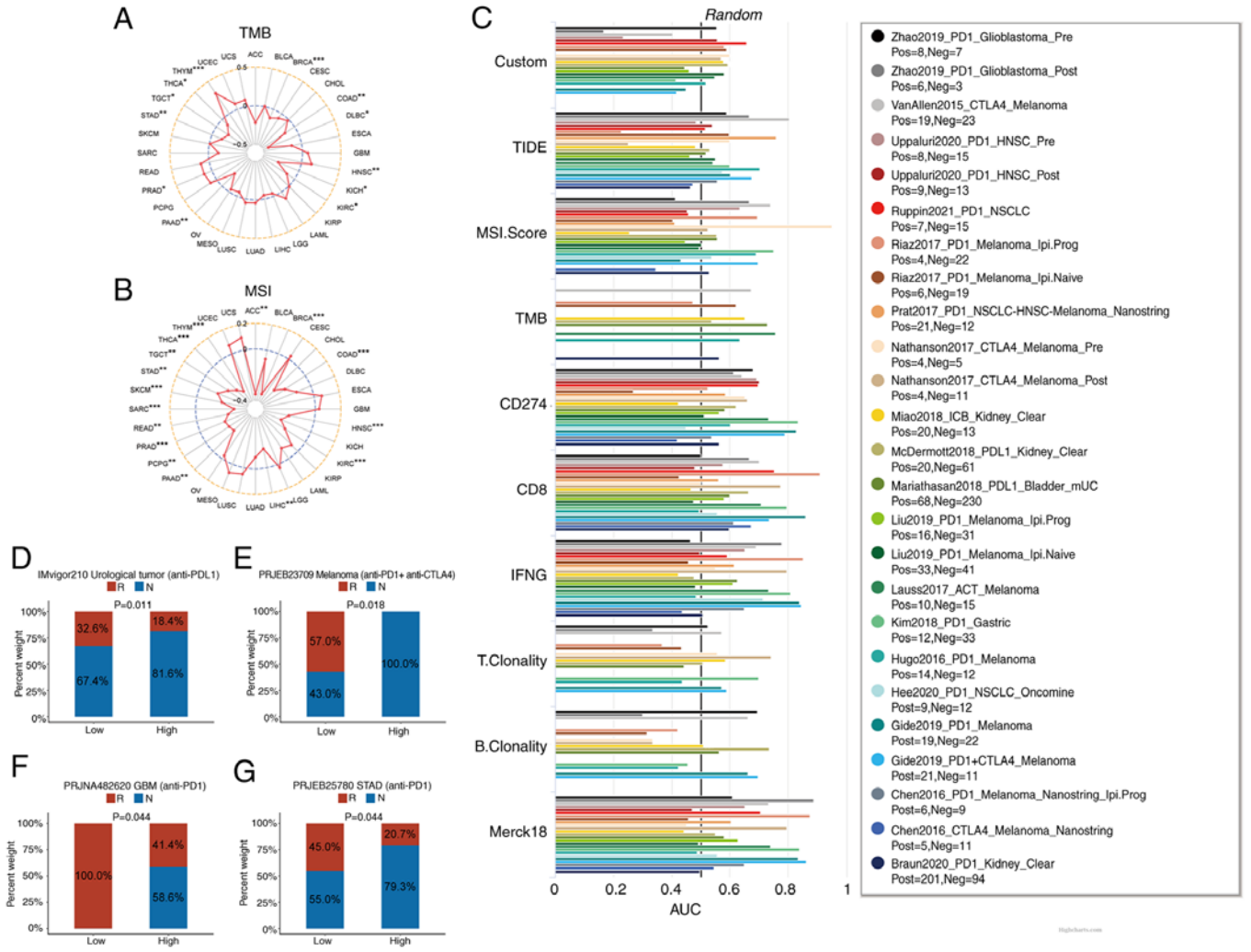

Figure 7. Predictive role of KMT2C in cancer immunotherapy. (A) The correlation between KMT2C expression and TMB in pan-cancer. (B) The correlation between KMT2C expression and MSI in pan-cancer. (C) The predictive value of KMT2C as a biomarker in immunotherapy cohorts. The objective response rates of low and high KMT2C expression subgroups of patients in the (D) IMvigor210, (E) PRJEB23709, (F) PRJNA482620 and (G) PRJEB25780 immunotherapy cohorts. *P<0.05, **P<0.01, ***P<0.001. AUC, area under the curve; R, response; N, no response; KMT2C, histone lysine N-methyltransferase 2C; TMB, tumor mutational burden; MSI, microsatellite instability; PD-1, programmed cell death protein 1.

348 patients with urological tumors who had been treated with anti-PD-L1 immunotherapy. The PRJEB23709 cohort included 91 patients with metastatic melanoma who had been treated with anti-programmed cell death protein 1 (PD-1) monotherapy or anti-PD-1 and anti-CTLA-4 in a combination immunotherapy. The PRJNA482620 cohort included the transcriptomic and clinical profiles of 34 patients with GBM who had been treated with anti-PD-1 immunotherapy. The PRJEB25780 cohort included data from 78 patients with metastatic gastric tumors, who had been treated with anti-PD-1 immunotherapy. These immunotherapy cohort datasets were used to evaluate the ability of KMT2C to predict the ORR. Patients with low KMT2C expression had higher ORRs following immunotherapy in all 4 cohorts (Fig. 7D-G). The ORR for patients with high KMT2C expression in the IMvigor210 cohort was 18.4% and the ORR for patients with low KMT2C expression was 32.6% (Fig. 7D). The association between KMT2C and the clinical response rates to immunotherapy drugs was also examined. In the PRJNA482620 dataset, the patients were treated with pembrolizumab or nivolumab. The response rate of patients with low KMT2C expression (100.0%) was significantly higher than that of patients with high KMT2C expression (41.4%) (Fig. 7F). In the GSE78220 dataset, patients were treated with pembrolizumab or nivolumab. The response rate of patients with low KMT2C expression (80.0%) was higher than that of patients with high KMT2C expression (45.5%) (Fig. S6B). In the PRJEB25780 dataset, patients were treated with pembrolizumab. The response rate of patients with low KMT2C expression (45.0%) was higher than that of patients with high KMT2C expression (20.7%) (Fig. 7G). These results implicated KMT2C expression as a potential biomarker of the clinical response to pembrolizumab or nivolumab. Tissue samples from 29 patients with kidney cancer were also analyzed and a significant positive correlation between KMT2C expression and PD-L1 expression was observed (Figs. S6C, S7 and S8). This was consistent with the results of the pan-cancer analysis. However, as there is no available KMT2C antibody with good specificity, there was a problem with high background signal in the immunohistochemistry results, which affected the conclusions to a certain extent.

KMT2C-mediated prediction of pan-cancer drug sensitivity. To date and to the best of our knowledge, no small molecule inhibitors that target KMT2C have been reported. Thus, potential inhibitors of the KMT2C-regulated signaling pathway were identified using the CMap dataset. High KMT2C expression was negatively correlated with the topoisomerase (TOP) I inhibitors, irinotecan and camptothecin, in 33 and 29 cancer types, respectively. KMT2C expression was negatively correlated with the TOP II inhibitor, mitoxantrone, in 26 cancer types. In addition, primaquine, a potent antimalarial agent, was also enriched in 25 cancer types (Fig. 8A). An analysis of a GDSC dataset (https://www.cancerrxgene.org/) found that KMT2C expression was significantly negatively correlated with several TOP I inhibitors (SN38, irinotecan and camptothecin), a TOP II inhibitor (mitoxantrone), several histone deacetylase (HDAC) inhibitors (ACY1215, belinostat, CAY10603, vorinostat, entinostat, panobinostat, trichostatin A and tubastatin A), DOT1-like histone H3K79 methyltransferase (DOT1L) inhibitors (EPZ004777 and EPZ5676) and a G9A nuclear histone lysine methyltransferase inhibitor (UNC0638) (Figs. 8B and S9A). These results indicated that these small molecule inhibitors may be suitable for treating tumors with high levels of KMT2C expression. In addition, it was found that KMT2C expression was significantly correlated with TOP I, HDAC 1-9, DOT1L and G9A expression, indicating that KMT2C interacted with these proteins via direct or indirect mechanisms (Fig. S9B). The antiproliferative effect of TOP I, HDAC, DOT1L and G9A inhibitors in different cancer cells *in vitro* was also verified. The result indicated that SN38 (TOP I inhibitor) and vorinostat (HDAC inhibitor) inhibited the proliferation of A549 and H1975 cells (Fig. S9C and D).

Cellular in vitro assays. The role of KMT2C in a variety of tumor cell lines has been previously studied, including breast, prostate and ovarian cancer cell lines (39-41). In addition, KMT2C mutations have been significantly associated with the metastasis of small-cell lung cancer (21), but the role of KMT2C in non-small cell lung cancer (NSCLC) metastasis has not, to the best of our knowledge, been studied. Therefore, the role of KMT2C in NSCLC was explored by knocking down KMT2C expression in A549 and H1975 cells using shRNA. The RT-qPCR and dot blot results showed that the expression of KMT2C in A549 and H1975 cells was significantly reduced following shRNA treatment (Figs. 9A, S10A and S10B). The reduction in KMT2C expression significantly improved the proliferation and migration of A549 cells in colony formation and wound healing assays, respectively (Fig. 9B-E). However, knocking down KMT2C expression reduced the proliferation of H1975 cells (Fig. S10C). These differing results may be related to the different expression levels of KMT2C in these cells (Fig. S10D).

Discussion

Immunotherapies using ICIs or adoptively transferred immune cells have revolutionized cancer treatment, especially for metastatic cancer (42,43), and patients previously considered as incurable can now achieve long-term remission and survival (44). Although immunotherapy can produce a lasting response, ICI monotherapy typically has an ORR of only ~20% for solid tumors, and numerous patients eventually developed drug resistance. A number of mechanisms, including intrinsic cancer cell factors and immunosuppressive cells, create a TME that is hostile to tumor-targeting immune cells (45,46). Consequently, researchers have begun to explore biomarkers to achieve precise immunotherapy. Biomarkers can screen patients who may benefit from immunotherapy and avoid unnecessary medical costs, hyper-progression and potentially severe toxicity in individuals who are unlikely to respond to treatment (47-49). However, the identification of effective and reliable biomarkers remains a significant challenge in immunotherapy. In the present study, the value of KMT2C in predicting response to ICI immunotherapy was investigated and it was discovered that KMT2C was a robust pan-cancer prognostic biomarker.

The pan-cancer expression of KMT2C was first evaluated and it was found that KMT2C was highly expressed in BRCA, CHOL, ESCA, GBM, KICH, LAML, LGG, PAAD, PRAD and STAD. In contrast, KMT2C expression was low in ACC, BLCA, CESC, COAD, LUAD, LUSC, OV, SKCM, TGCT, THCA, THYM, UCEC and UCS. Paired expression analyses revealed that KMT2C expression was high in CHOL, COAD, LIHC, KICH and THCA, suggesting that KMT2C plays an important role in the development and progression of these cancer types. The pan-cancer prognostic value of KMT2C was also evaluated using univariate Cox regression and Kaplan-Meier analyses. These two methods yielded consistent results. KMT2C was a protective factor for patients with KIRC and OV, but a risk factor for patients with LUSC and UVM, indicating that KMT2C might have different roles in different cancer types.

Tumor-infiltrating immune cells have critical roles in the eradication of tumors, and cancer cells can inhibit immune cell infiltration by reshaping the TME (50,51). In the present study, the GSEA results suggested that KMT2C expression was significantly negatively correlated with immune activation, such as the TNF-α, IFN-γ and IFN-α pro-inflammatory responses and allograft rejection, indicating that tumors with high levels of KMT2C were poorly immunogenic. Angiogenesis is another cancer hallmark that is necessary for tumor cell survival and plays an important role in tumor growth, invasion and metastasis (52). In the present study, it was demonstrated that KMT2C expression was significantly positively correlated with the neovascularization process, angiogenesis and the VEGFA/VEGFR2 signaling pathway. Tumor angiogenesis is a marker of cancer progression, and there is growing evidence that it also causes immunosuppression and evasion of antitumor immunity. Angiogenesis factors are known to directly or indirectly inhibit T cell development and function, promote T cell exhaustion by upregulating immune checkpoints, inhibit DC maturation, regulate macrophage polarization and increase the number of intratumoral regulatory T cells and MDSCs (53-55). In addition, tumor vascular dysfunction leads to insufficient blood perfusion and oxygenation, in turn leading to tumor hypoxia, which produces various immunosuppressive effects (56). The results of the present study suggested that KMT2C may promote tumor vascularization by regulating the expression of angiogenesis factors such as VEGF and FGF. Thus, targeting KMT2C may be a good way to inhibit vascularization.

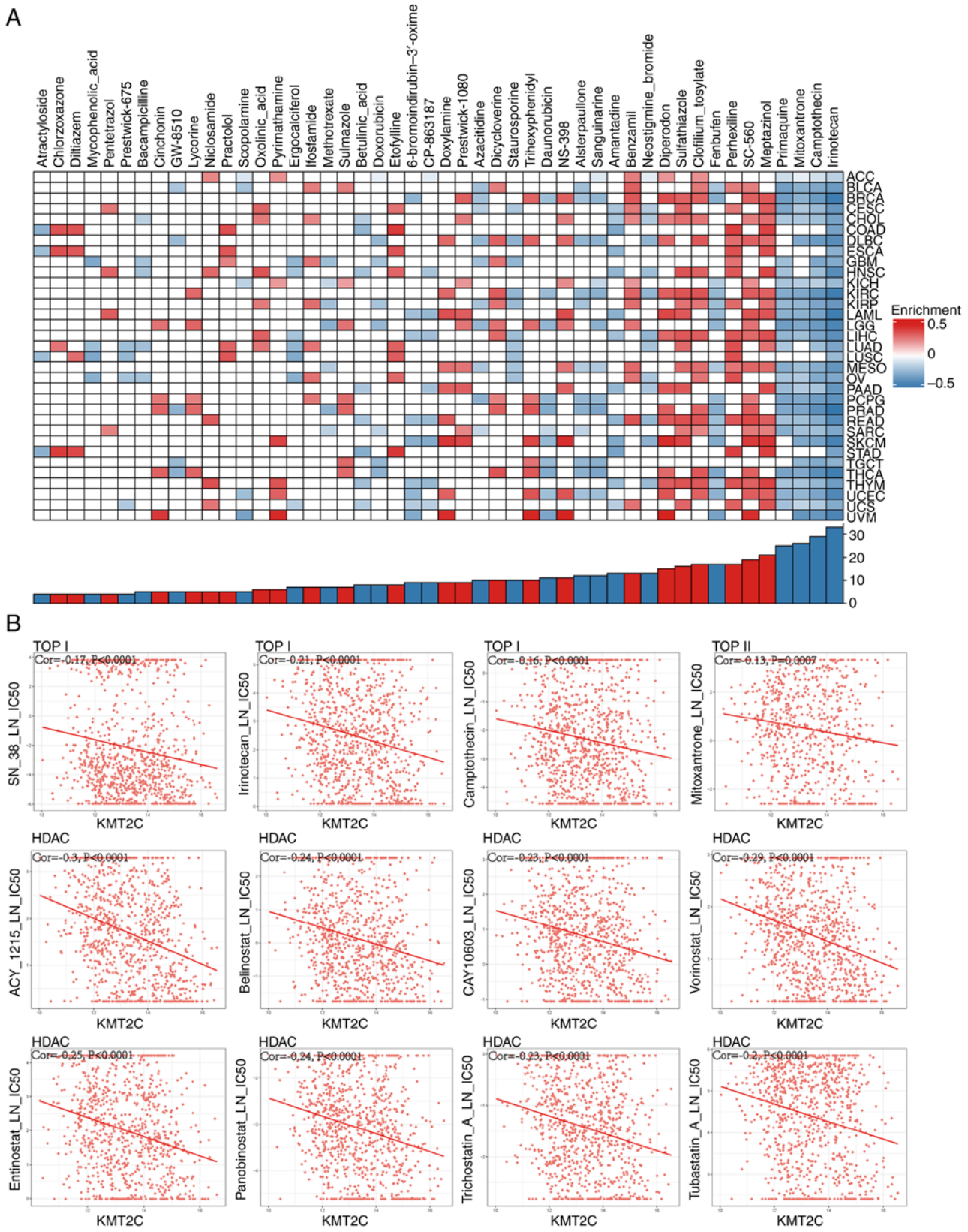

Figure 8. Prediction of anti-cancer drug sensitivity based on KMT2C expression in pan-cancer. (A) Correlations between KMT2C expression and drug sensitivity were calculated using CMap and (B) GDSC databases. KMT2C, histone lysine N-methyltransferase 2C; HDAC, histone deacetylase; TOP, topoisomerase.

In the present study, the association between KMT2C expression and the intratumoral infiltration of various immune cells that play critical and diverse roles in tumor suppression was investigated. Cytotoxic $CD8^+$ T cells recognize and kill tumor cells (57). Monocytes play key roles in the maintenance of homeostasis, pathogen recognition, clearance and

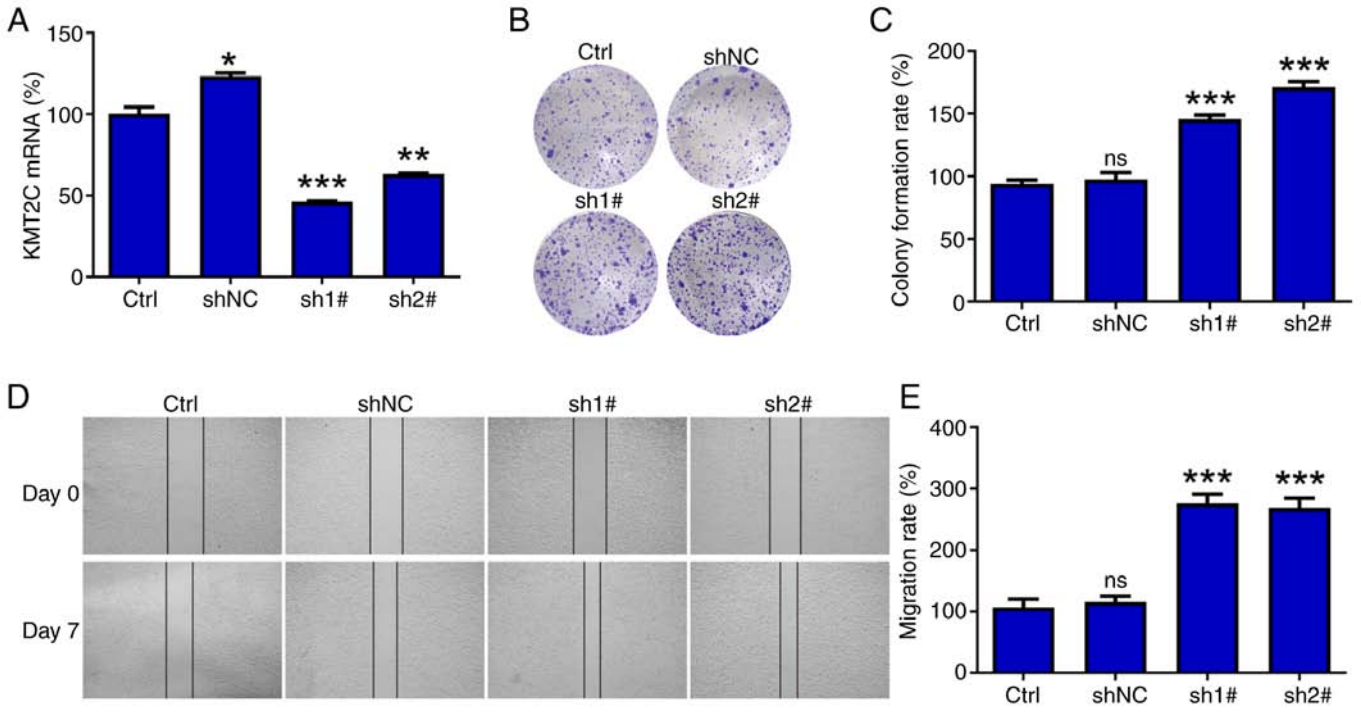

Figure 9. Cellular *in vitro* assays. (A) The transfection efficiency of sh-KMT2C in A549 cells was verified by reverse transcription-quantitative PCR. (B) Representative images of colony formation of A549 cell and A549 shKMT2C cell. (C) Knocking down KMT2C expression increased the colony formation ability of A549 cells. (D) Representative images of migration of A549 cell and A549 shKMT2C cell. (E) Knocking down KMT2C expression promoted the migration capacity of A549 cells. *P<0.05, **P<0.01, ***P<0.001. Ctrl, control; KMT2C, histone lysine N-methyltransferase 2C; NC, negative control; ns, not significant; sh, short hairpin.

inflammation (58). NK cells have antitumor functions and are involved in immune regulation (59). Macrophages are important autologous immune cells that participate in the clearance of infected and tumor-transformed cells and in immunomodulation (60). CAFs are an important component of the TME and have multiple functions such as extracellular matrix remodeling, regulation of metabolism and angiogenesis, and interaction with cancer cells and infiltrating immune cells. CAFs promote tumorigenesis, tumor development, and resistance to a various therapeutic strategies, including chemotherapy, radiotherapy, targeted therapy, antiangiogenic therapy, immunotherapy and endocrine therapy (61). ECs also have an important role in tumor angiogenesis. Tumor-associated neutrophils enhance the proliferation of tumor cells by releasing neutrophil extracellular traps (62). The results of the present study indicated that KMT2C expression was negatively correlated with enrichment of infiltrated $CD8^+$ T cells, monocytes, NK cells and macrophages in most cancer types, and positively correlated with the presence of CAFs, ECs, neutrophils and Tregs in the TME. In addition, it was found that KMT2C levels were positively correlated with the expression of inhibitory immune genes, such as CD274, KDR and IDO1. Collectively, these results suggested that KMT2C expression could maintain the immunosuppressive TME by regulating immune cell infiltration.

The predictive value of KMT2C was then evaluated in 25 immunotherapy cohorts and it was found that KMT2C exhibited a higher predictive value than TMB, T.Clonality and B.Clonality. By evaluating whether KMT2C could predict the ORR in patients with cancer receiving immunotherapy, it was found that patients with low KMT2C expression had a higher ORR following immunotherapy than those with high KMT2C expression. ORRs of patients in the IMvigor210, PRJEB23709, PRJNA482620 and PRJEB25780 cohorts were 22.8, 53.8, 50.0 and 26.9%, respectively. The respective ORRs of patients with low KMT2C expression were 32.6, 57.0, 100.0 and 45.0%, respectively. These results indicated that KMT2C may effectively predict the response to immunotherapy. The correlation between KMT2C and PD-L1 expression in kidney tumors was also verified, and it was found that KMT2C expression was significantly and positively correlated with PD-L1 expression. As one of the most important immune checkpoints, PD-L1 can be induced by inflammatory cytokines, including IFN, TNF-α and VEGF, in addition to constitutively low expression in Antigen-presenting cells (APCs) and a variety of non-hematopoietic cells (63,64). Tumor cells and tumor-associated antigen presenting cells highly express PD-L1 in the TME, whereas tumor-infiltrating lymphocytes express PD-1 in response to long-term tumor antigen stimulation. The combination of PD-L1 and PD-1 can induce apoptosis, incapacitation and depletion of T cells, and then inhibit the activation, proliferation and antitumor function of tumor antigen-specific $CD8^+$ T cells, leading to tumor immune escape (65). KMT2C is a methyltransferase that regulates gene expression via epigenetic modifications (66). Therefore, tumor cells may regulate the expression of PD-L1 through KMT2C, thereby facilitating immune escape. This may also explain why patients with low KMT2C expression have better treatment outcomes when undergoing immunotherapy.

Since KMT2C is a DNA damage repair regulator, targeting KMT2C could enhance the antitumor effects of chemotherapeutic drugs, particularly those that induce DNA damage. However, to the best of our knowledge, no KMT2C inhibitors

have been developed to date. In the present study, CMap and GDSC datasets were used to analyze the association between drug sensitivity and KMT2C expression. TOP I, HDAC, DOT1L and G9A inhibitor sensitivities were significantly correlated with KMT2C expression. The drug sensitivity test results also showed that TOP I (SN38) and HDAC (vorinostat) inhibitors potently inhibited the proliferation of A549 and H1975 cells.

In conclusion, in the present study, a pan-cancer data analysis revealed that KMT2C was a protective factor for patients with KIRC and OV, but a risk factor for patients with LUSC and UVM. High KMT2C expression was negatively correlated with immune cell infiltration, immune stimulatory regulators, TMB and MSI in various cancer types. In addition, patients with low KMT2C levels showed higher ORRs following immunotherapy. Taken together, these findings demonstrated that KMT2C may be a biomarker for predicting response to immunotherapy. However, the present study had certain limitations, such as the relatively small sample size in the immunotherapy cohort, which may have led to inevitable systematic bias and affected the resulting conclusions. Therefore, the role of KMT2C in the context of cancer immunotherapy requires further validation using larger datasets. Furthermore, the use of only lung cancer cell lines was another limitation of the present study and thus, more studies including additional cell lines are required in the future.

Acknowledgements

Not applicable.

Funding

This work was supported by The National Natural Science Foundation of China (grant no. 81972040), The Anhui Provincial Natural Science Foundation (grant nos. 2108085MH321 and 2108085QH379), The Research Fund of Anhui Medical University (grant no. 2020xkj013) and the Foundation of Science and Technology Department of Anhui Province of China (grant no. KJ2021A0313).

Availability of data and materials

The data generated in the present study may be requested from the corresponding author.

Authors' contributions

WLW, XSL and RL designed the research. WC, LC, YWX, MQW, ZYC, ZTW, YQW, JJX and YW performed the experiments. WC and WLW wrote the manuscript. MQW, ZYC, ZTW, YQW and JJX provided experiment materials. WLW revised the manuscript. All authors have read and approved the final manuscript. WLW and XSL confirm the authenticity of all the raw data.

Ethics approval and consent to participate

Paraffin-embedded kidney tumor tissue samples were obtained from patients treated at the Second Affiliated Hospital of Anhui Medical University (Hefei, China), with written informed consent. All experiments were approved by The Medical Ethics Committee of the Second Affiliated Hospital of Anhui Medical University (approval no. 81220282).

Patient consent for publication

Not applicable.

Competing interests

The authors declare that they have no competing interests.

References

1. Kubli SP, Berger T, Araujo DV and Mak L: Beyond immune checkpoint blockade: Emerging immunological strategies. Nat Rev Drug Discov 20: 899-819, 2021.
2. He X and Xu C: Immune checkpoint signaling and cancer immunotherapy. Cell Res 30: 660-669, 2020.
3. Huang Q, Lei Y, Li X, Guo F and Liu M: A Highlight of the mechanisms of immune checkpoint blocker resistance. Front Cell Dev Biol 8: 580140, 2020.
4. Waldman AD and Lenardo J: A guide to cancer immunotherapy: From T cell basic science to clinical practice. Nat Rev Immunol 20: 651-668, 2020.
5. Kruger S, Ilmer M, Kobold S, Cadilha B, Endres S, Ormanns S, Schuebbe G, Renz BW, D'Haese JG, Schloesser H, *et al*: Advances in cancer immunotherapy 2019-latest trends. J Exp Clin Cancer Res 38: 268, 2019.
6. Ribas A and Wolchok JD: Cancer immunotherapy using checkpoint blockade. Science 359: 1350-1355, 2018.
7. Darvin P, Toor S and Elkord V: Immune checkpoint inhibitors: Recent progress and potential biomarkers. Exp Mol Med 50: 1-11, 2018.
8. Acevedo J, Kimbrough E and Lou Y: Next generation of immune checkpoint inhibitors and beyond. J Hematol Oncol 14: 45, 2021.
9. Johnson D, Nebhan C, Moslehi J and Balko J: Immune-checkpoint inhibitors: Long-term implications of toxicity. Nat Rev Clin Oncol 19: 254-267, 2022.
10. Franzin R, Netti G, Spadaccino F, Porta C, Gesualdo L, Stallone G, Castellano G and Ranieri E: The use of immune checkpoint inhibitors in oncology and the occurrence of AKI: Where do we stand? Front Immunol 11: 574271, 2020.
11. Wright J, Powers A and Johnson D: Endocrine toxicities of immune checkpoint inhibitors. Nat Rev Endocrinol 17: 389-399, 2021.
12. Rao R and Dou Y: Hijacked in cancer: The KMT2 (MLL) family of methyltransferases. Nat Rev Cancer 15: 334-346, 2015.
13. Park K and Kim J: Transcriptional regulation by the KMT2 histone H3K4 methyltransferases. Biochim Biophys Acta Gene Regul Mech 1863: 194545, 2020.
14. Zhai X and Brownell J: Biochemical perspectives on targeting KMT2 methyltransferases in cancer. Trends Pharmacol Sci 42: 688-699, 2021.
15. Zhu J, Liu Z, Liang X, Wang L, Wu D, Mao W and Shen D: A Pan-Cancer study of KMT2 family as therapeutic targets in cancer. J Oncol 2022: 3982226, 2022.
16. Shen E, Shulha H, Weng Z and Akbarian S: Regulation of histone H3K4 methylation in brain development and disease. Philos Trans R Soc Lond B Biol Sci 369: 20130514, 2014.
17. Bochyńska A, Firzlaff J and Lüscher B: Modes of Interaction of KMT2 Histone H3 Lysine 4 Methyltransferase/COMPASS complexes with chromatin. Cells 7: 17, 2018.
18. Rampias T, Karagiannis D, Avgeris M, Polyzos A, Kokkalis A, Kanaki Z, Kousidou E, Tzetis M, Kanavakis E, Stravodimos K, *et al*: The lysine-specific methyltransferase KMT2C/MLL3 regulates DNA repair components in cancer. EMBO Rep 20: e46821, 2019.
19. Chang A, Liu L, Ashby J, Wu D, Chen Y, O'Neill SS, Huang S, Wang J, Wang G, Cheng D, *et al*: Recruitment of KMT2C/MLL3 to DNA damage sites mediates DNA damage responses and regulates PARP inhibitor sensitivity in cancer. Cancer Res 81: 3358-3373, 2021.

20. Mendiratta G, Ke E, Aziz M, Liarakos D, Tong M and Stites E: Cancer gene mutation frequencies for the U.S. population. Nat Commun 12: 5961, 2021.
21. Na F, Pan X, Chen J, Chen X, Wang M, Chi P, You L, Zhang L, Zhong A, Zhao L, *et al*: KMT2C deficiency promotes small cell lung cancer metastasis through DNMT3A-mediated epigenetic reprogramming. Nat Cancer 3: 753-767, 2022.
22. Chen X, Zhang G, Chen B, Wang Y, Guo L, Cao L, Ren C, Wen L and Liao N: Association between histone lysine methyltransferase KMT2C mutation and clinicopathological factors in breast cancer. Biomed Pharmacother 116: 108997, 2019.
23. Zhang P and Huang Y: Genomic alterations in KMT2 family predict outcome of immune checkpoint therapy in multiple cancers. J Hematol Oncol 14: 39, 2021.
24. Zhang R, Wu H, Xu M and Xie X: KMT2A/C mutations function as a potential predictive biomarker for immunotherapy in solid tumors. Biomark Res 8: 71, 2020.
25. Tu Z, Ouyang Q, Long X, Wu L, Li J, Zhu X and Huang K: Protein Disulfide-Isomerase A3 is a robust prognostic biomarker for cancers and predicts the immunotherapy response effectively. Front Immunol 13: 837512, 2022.
26. Sun D, Wang J, Han Y, Dong X, Ge J, Zheng R, Shi X, Wang B, Li Z, Ren P, *et al*: TISCH: A comprehensive web resource enabling interactive single-cell transcriptome visualization of tumor microenvironment. Nucleic Acids Res 49: D1420-D1430, 2021.
27. Lamb J: The connectivity map: A new tool for biomedical research. Nat Rev Cancer 7: 54-60, 2007.
28. Barretina J, Caponigro G, Stransky N, Venkatesan K, Margolin A, Kim S, Wilson CJ, Lehár J, Kryukov GV, Sonkin D, *et al*: The cancer cell line encyclopedia enables predictive modelling of anticancer drug sensitivity. Nature 483: 603-607, 2012.
29. Jin Y, Wang Z, He D, Zhu Y, Chen X and Cao K: Identification of novel subtypes based on ssGSEA in immune-related prognostic signature for tongue squamous cell carcinoma. Cancer Med 10: 8693-8707, 2021.
30. Liu J, Liu Q, Shen H, Liu Y, Wang Y, Wang G and Du J: Identification and validation of a three Pyroptosis-Related lncRNA signature for prognosis prediction in lung adenocarcinoma. Front Genet 13: 838624, 2022.
31. Mariathasan S, Turley S, Nickles D, Castiglioni A, Yuen K, Wang Y, Kadel EE III, Koeppen H, Astarita JL, Cubas R, *et al*: TGFβ attenuates tumour response to PD-L1 blockade by contributing to exclusion of T cells. Nature 554: 544-548, 2018.
32. Xiong D, Wang Y and You M: A gene expression signature of TREM2hi macrophages and γδ T cells predicts immunotherapy response. Nat Commun 11: 5084, 2020.
33. Zhao J, Chen A, Gartrell R, Silverman A, Aparicio A, Chu T, Bordbar D, Shan D, Samanamud J, Mahajan A, *et al*: Immune and genomic correlates of response to anti-PD-1 immunotherapy in glioblastoma. Nat Med 25: 462-469, 2019.
34. Kim S, Cristescu R, Bass A, Kim M, Odegaard J, Kim K, Liu XQ, Sher X, Jung H, Lee M, *et al*: Comprehensive molecular characterization of clinical responses to PD-1 inhibition in metastatic gastric cancer. Nat Med 24: 1449-1458, 2018.
35. Amin MB, Greene FL, Edge SB, Compton CC, Gershenwald JE and Brookland R: The Eighth Edition AJCC Cancer Staging Manual: Continuing to build a bridge from a population-based to a more 'personalized' approach to cancer staging. CA Cancer J Clin 67: 93-99, 2017.
36. Livak KJ and Schmittgen TD: Analysis of relative gene expression data using real-time quantitative PCR and the 2(-Delta Delta C(T)) method. Methods 25: 402-408, 2001.
37. Wang WL, Jiang ZR, Hu C, Chen C, Hu ZQ, Wang AL, Wang L, Liu J, Wang WC and Liu QS: Pharmacologically inhibiting phosphoglycerate kinase 1 for glioma with NG52. Acta Pharmacol Sin 42: 633-640, 2021.
38. Pan D, Kobayashi A, Jiang P, Ferrari de Andrade L, Tay RE, Luoma AM, Tsoucas D, Qiu X, Lim K, Rao P, *et al*: A major chromatin regulator determines resistance of tumor cells to T cell-mediated killing. Science 359: 770-775, 2018.
39. Gala K, Li Q, Sinha A, Razavi P, Dorso M, Sanchez-Vega F, Chung YR, Hendrickson R, Hsieh JJ, Berger M, *et al*: KMT2C mediates the estrogen dependence of breast cancer through regulation of ERα enhancer function. Oncogene 37: 4692-4710, 2018.
40. Xiong W, Deng H, Huang C, Zen C, Jian C, Ye K, Zhong Z, Zhao X and Zhu L: MLL3 enhances the transcription of PD-L1 and regulates anti-tumor immunity. Biochim Biophys Acta Mol Basis Dis 1865: 454-463, 2019.
41. Zheng J, Wang C, Gao C, Xiao Q, Huang C, Wu M and Li LY: MLL3 suppresses tumorigenesis through regulating TNS3 enhancer activity. Cell Death Dis 12: 364, 2021.
42. Sugie T: Immunotherapy for metastatic breast cancer. Chin Clin Oncol 7: 28, 2018.
43. Wrobel P and Ahmed S: Current status of immunotherapy in metastatic colorectal cancer. Int J Colorectal Dis 34: 13-25, 2019.
44. Sharma P and Allison J: The future of immune checkpoint therapy. Science 348: 56-61, 2015.
45. Vesely M, Zhang T and Chen L: Resistance mechanisms to Anti-PD cancer immunotherapy. Annu Rev Immunol 40: 45-74, 2022.
46. Schoenfeld A and Hellmann M: Acquired resistance to immune checkpoint inhibitors. Cancer Cell 37: 443-455, 2022.
47. Chan T, Yarchoan M, Jaffee E, Swanton C, Quezada S, Stenzinger A and Peter S: Development of tumor mutation burden as an immunotherapy biomarker: Utility for the oncology clinic. Ann Oncol 30: 44-56, 2019.
48. Walk E, Yohe S, Beckman A, Schade A, Zutter M, Pfeifer J and Berry AB; College of American Pathologists Personalized Health Care Committee: The cancer immunotherapy biomarker testing landscape. Arch Pathol Lab Med 144: 706-724, 2020.
49. Chang L, Chang M, Chang H and Chang F: Microsatellite instability: A predictive biomarker for cancer immunotherapy. Appl Immunohistochem Mol Morphol 26: e15-e21, 2018.
50. Chen Y, Zhao B and Wang X: Tumor infiltrating immune cells (TIICs) as a biomarker for prognosis benefits in patients with osteosarcoma. BMC Cancer 20: 1022, 2020.
51. Jiang B, Mason J, Jewett A, Liu M, Chen W, Qian J, Ding Y, Ding S, Ni M, Zhang X and Man YG: Tumor-infiltrating immune cells: Triggers for tumor capsule disruption and tumor progression?. Int J Med Sci 10: 475-497, 2013.
52. Li T, Kang G, Wang T and Huang H: Tumor angiogenesis and anti-angiogenic gene therapy for cancer. Oncol Lett 16: 687-702, 2018.
53. Liu ZL, Chen HH, Zheng LL, Sun LP and Shi L: Angiogenic signaling pathways and anti-angiogenic therapy for cancer. Signal Transduct Target Ther 8: 198, 2023.
54. Fang JW, Lu Y, Zheng JY, Jiang XC, Shen HX, Shang X, Lu Y and Fu P: Exploring the crosstalk between endothelial cells, immune cells, and immune checkpoints in the tumor microenvironment: New insights and therapeutic implications. Cell Death Dis 14: 586, 2023.
55. Zhu L, Yu X, Wang L, Liu J, Qu Z, Zhang H, Li L, Chen J and Zhou Q: Angiogenesis and immune checkpoint dual blockade in combination with radiotherapy for treatment of solid cancers: Opportunities and challenges. Oncogenesis 10: 47, 2021.
56. Guo FF and Cui JW: Anti-angiogenesis: Opening a new window for immunotherapy. Life Sci 258: 118163, 2020.
57. Iwahori K: Cytotoxic CD8+ lymphocytes in the tumor microenvironment. Adv Exp Med Biol 1224: 53-62, 2020.
58. Ugel S, Canè S, Sanctis F and Bronte V: Monocytes in the tumor microenvironment. Annu Rev Pathol 16: 93-122, 2021.
59. Wu S, Fu T, Jiang Y and Shao Z: Natural killer cells in cancer biology and therapy. Mol Cancer 19: 120, 2020.
60. Li X, Liu R, Su X, Pan Y, Han X, Shao C and Shi Y: Harnessing tumor-associated macrophages as aids for cancer immunotherapy. Mol Cancer 18: 177, 2020.
61. Liao Z, Tan Z, Zhu P and Tan N: Cancer-associated fibroblasts in tumor microenvironment-Accomplices in tumor malignancy. Cell Immunol 343: 103729, 2021.
62. Kim J and Bae J: Tumor-Associated macrophages and neutrophils in tumor microenvironment. Mediators Inflamm 2016: 6058147, 2016.
63. Dirix V, Corbière V, Thomas CW, Selis E, Allard S, Hites M, Aerts L, Giese T and Mascart F: Blood tolerogenic monocytes and low proportions of dendritic cell subpopulations are hallmarks of human tuberculosis. J Leukoc Biol 103: 945-954, 2018.
64. Safi M, Ahmed H, Al-Azab M, Xia YL, Shan X, Al-Radhi M, Al-Danakh A, Shopit A and Liu J: PD-1/PDL-1 inhibitors and cardiotoxicity; molecular, etiological and management outlines. J Adv Res 29: 45-54, 2020.
65. Hashimoto M, Kamphorst AO, Im SJ, Kissick HT, Pillai RN, Ramalingam SS, Araki K and Ahmed R: CD8 T cell exhaustion in chronic infection and cancer: Opportunities for interventions. Annu Rev Med 69: 301-318, 2018.
66. Yang HS, Cui W and Wang LH: Epigenetic synthetic lethality approaches in cancer therapy. Clin Epigenetics 11: 136, 2019.